Giant SALR cluster reproduction, with implications for their chemical evolution

Giant SALR cluster reproduction, with implications for their chemical evolution

M.B. Sweatman

School of Engineering, University of Edinburgh, King's Buildings, Mayfield Road, Edinburgh, Scotland, UK. EH9 3FB

Martin.sweatman@ed.ac.uk

25th August 2017

Giant SALR cluster reproduction, with implications for their chemical evolution

Particles with SALR (short-range attraction and long-range repulsion) interactions are common to many physical systems, especially biological and soft matter, yet their behaviour is still not completely understood. Using Monte Carlo simulations and a thermodynamic model, it is shown here that giant SALR clusters can grow and reproduce in these fluids. Giant cluster growth and reproduction should therefore be common to a wide range of natural and synthetic systems under suitable conditions. If, in addition, cluster fitness selection occurs then chemical evolution of giant SALR cluster might be observed in suitable systems.

Keywords: SALR, clusters, mesoscale, soft matter, reproduction, nucleation, competing interactions

I. SALR fluids

SALR fluids comprise particles with short-range attractions and long-range repulsions[1-3]. These model potentials are often used to represent particles in a wide range of physical systems, from nuclear[4,5] to soft matter[6-26]. However, even the *equilibrium* behaviour of relatively simple one-component SALR fluids is not completely understood[27-29]. There is therefore great incentive to study the equilibrium and non-equilibrium behaviour of model SALR fluids, and their mixtures with other particles, given the wide range of applications.

Much work in the soft matter domain has focussed on non-equilibrium aspects associated with kinetic arrest and network forming in SALR systems with very strong and short-range attractions, relevant to some biological macromolecule[16,21] and colloidal

dispersions[7,20,24]. More recently, the equilibrium phase behaviour of systems with weaker interactions, that do not undergo kinetic arrest and instead display giant clusters, has come into focus[3,28-32], as it is recognised that these interactions might be suitable for smaller solutes, and in any case this equilibrium behaviour will drive the behaviour of SALR dispersions that do become kinetically frustrated.

As a pertinent example, consider the following problem in cell biology. It is generally thought that membrane-less organelles inside cells are generated via classical nucleation[33]. However, the stable existence of multiple organelles of the same type within a cell suggests that classical nucleation, by itself, is insufficient as these organelles would be expected to combine into one domain. However, their stability as multiple independent clusters might be explained in terms of giant SALR clusters.

Recent simulation[3] and theoretical work[27-29,32,34,35] has established that the equilibrium phase behaviour is rather complex, yet quite similar to that of aqueous surfactants in some respects. That is, giant micelle-like clusters (forming a 'cluster fluid') can occur at low solute densities higher than the 'critical cluster concentration' (CCC), while modulated fluids with a range of geometrical structures can occur at high solute densities. Moreover, the SALR phase diagram is now known to include a first order phase transition from a cluster vapour phase to a condensed cluster phase (solid or liquid) driven by depletion interactions[28,29], and it is argued that the cluster-vapour to cluster-liquid transition should only exist within a very narrow range of system parameters[29].

Simulations of these fluids have tended to focus on the formation of giant SALR clusters in systems with a fixed number of particles (the NVT, or canonical ensemble) at high super-saturations such that clusters form quickly from an initially disordered dispersion. Cluster reproduction has not been observed in these simulations. Here, we

find that by very slowly increasing the number of particles in the system such that it remains at, or very close to, equilibrium, these systems display giant clusters that grow and reproduce within a particular range of model parameters.

This work is organised as follows. We introduce the SALR model potential in the next section. Then we describe and apply a thermodynamic model to analyse two routes to new cluster generation, i.e. nucleation and reproduction. Following this, we perform suitable Monte Carlo simulations to check results predicted by this theory. Finally, we summarize the work and consider its likely implications for giant SALR cluster evolution.

II. The SALR model

The SALR model potential is usually employed as an 'effective' potential between particles. Focussing on soft matter, the SALR potential is often employed to model the pairwise interaction between biological macromolecule, polyelectrolyte, nanoparticle or colloidal solutes in solution. The solvent is not modelled explicitly, i.e. the average effect of the solvent is taken into account through definition of the SALR potential. Normally, SALR interactions are defined in addition to a particle core, which prevents particle overlaps;

$$\phi(r) = \phi_{core}(r) + \phi_{SALR}(r) \qquad (1)$$

where r is the distance between a pair of particles. In this work, without loss of generality, the core is modelled as a hard sphere with diameter d, while a 2-Yukawa potential is employed to model short-range attractions and long-range repulsions;

$$\beta\phi\ (x) = \phi_{HS}(x) + \phi_{2Y}(x) = \begin{cases} \infty & ; \quad x < 1 \\ -A_a \exp(-z_a(x-1))/x + A_r \exp(-z_r(x-1))/x & ; \quad x \geq 1 \end{cases} \tag{2}$$

where $x = r/d$ and $\beta = 1/k_BT$, with k_B as Boltzmann's constant and T the temperature. The dimensionless SALR parameters A_a, A_r, z_a and z_r (all positive) control the magnitude and range of interactions beyond the core. In the following, dimensionless reduced units are used by comparing energies to k_BT and lengths to d.

Short-range attractions can represent a wide variety of solute aggregation mechanisms, from van der Waals interactions to depletion and solvophobic interactions. Long-range repulsions usually represent a screened-coulomb repulsion arising from like-charged solutes in the charge-neutralising background solvent. Thus, any particle that becomes charged in solution, for example through protonation or de-protonation, exhibits an SALR interaction with other like-charged solutes provided the counter-ion is very soluble, as is often the case in aqueous solutions. Therefore, SALR interactions are suitable for describing the effective interaction between a vast range of solutes in solution, including many biological molecules (both small ones like nucleobases and macromolecules like DNA), polyelectrolytes, many nanoparticles and charged colloids.

Giant SALR clusters occur at thermodynamic equilibrium when the short-ranged attractive and long-ranged repulsive interactions nearly balance and the overall system concentration is sufficiently high, i.e. above the 'critical cluster concentration', or CCC. An equilibrium phase diagram for the cluster fluid, predicted on the basis of a statistical thermodynamic model (essentially, a kind of coarse-grained density functional theory), is proposed in earlier work[28]. We should, therefore, expect to find cluster phases, or mesophases as they are sometimes called, in a very wide range of solutions, from simple fluid mixtures, to biological and colloidal solutions. In many cases they will be difficult to observe directly, unless the particle size is sufficiently large, for example in colloidal dispersions.

III. A thermodynamic model for giant SALR clusters

To understand giant SALR cluster reproduction behaviour it is instructive to first examine a thermodynamic model of the SALR fluid. The model described in reference [28] is suitable for these systems. Indeed, using it, a novel first order phase transition was predicted, from cluster vapour to a condensed cluster phase, and later confirmed to exist in Monte Carlo simulations[29]. The model is described fully in that earlier work, and therefore only described briefly here.

It relates the properties of the cluster system to the properties of the constituent particles via four independent parameters that describe the state of the cluster fluid, ρ_b = overall fluid density, ρ_c = density of clusters, ρ_l = liquid-like cluster body density, and d_c = cluster diameter. Clusters are modelled as spherical droplets with uniform liquid-like densities dispersed within a vapour-like background fluid. The energy density, u_c, is obtained from the energy equation with an approximation for the radial distribution function defined in terms of the state parameters. The entropy density, s_c, is approximated using a suitable combination of hard sphere terms. Thus the cluster fluid free energy density is expressed as

$$
\begin{aligned}
& f_c = u_c - Ts_c = f_{self} + f_{mix} \\
& \approx \int d\mathbf{r}' \phi_{SALR}(|\mathbf{r}-\mathbf{r}'|;d)\frac{\rho_c}{2} g_{HS}(|\mathbf{r}-\mathbf{r}'|;d,\rho_l)\int d\mathbf{R}\, P_c(\mathbf{r}-\mathbf{R})P_c(\mathbf{r}'-\mathbf{R}) - T\varphi s_{HS}(d,\rho_l) + k_B T\rho_c \ln\left(\frac{6M}{\rho_l}\sqrt{\frac{\pi(M-1)^3}{1000}}\right) \\
& + \int d\mathbf{r}' \phi_{SALR}(|\mathbf{r}-\mathbf{r}'|)\sum_{ij}\frac{\rho_i\rho_j}{2}\int d\mathbf{R}d\mathbf{R}'\, P_i(\mathbf{r}-\mathbf{R})g_{ij}(|\mathbf{R}-\mathbf{R}'|)P_j(\mathbf{r}'-\mathbf{R}') - T\left(s_{HS}(d_c^{eff},\rho_c) + \xi s_{HS}(d,\rho_g)\right)
\end{aligned}
\qquad (3)
$$

The first three terms on the right constitute the 'self' free energy density of clusters, where g_{HS} is the hard sphere radial distribution function, $P_c(r) = \rho_l\Theta(|r_c - \mathbf{r}|)$ is the cluster density distribution where $r_c = d_c/2$ and Θ is the Heaviside step function, and s_{HS} is the entropy density of hard spheres. Also, $\varphi = \rho_c\pi d_c^3/6$ is the volume fraction of

clusters and $M = \rho_l \pi d_c^3/6$ is the average number of particles per cluster. The last two terms on the right account for the free energy density of the mixture of clusters and dispersed particles where i,j stand for cluster (c) or vapour (v) , with $P_v(r) = \delta(r)$ and $\xi = 1 - \varphi$. The effective cluster diameter is determined from the Barker-Henderson route

$$d_c^{eff} = r_{cc}^{\min} + \int_{r_{cc}^{\min}}^{\infty} dr\,(1 - \exp(-\beta U_{cc}^{eff}(r))) \qquad (4)$$

where U_{cc}^{eff} is the effective cluster – cluster interaction, and the remaining radial distribution functions are defined via

$$\begin{aligned} g_{cc}(r) &= \begin{cases} \exp(-\beta U_{cc}^{eff}(r)) & ; \quad r > r_{cc}^{\min} \\ 0 & ; \quad r < r_{cc}^{\min} \end{cases} \\ g_{vc}(r) &= \begin{cases} g_{vc}^{mix}(r;\rho_v,d,\rho_c,d_c)\exp(-\beta U_{vc}^{eff}(r)) & ; \quad r > r_{vc}^{\min} \\ g_{vc}^{mix}(r;\rho_v,d,\rho_c,d_c)\exp(-\beta U_{vc}^{eff}(r_{vc}^{\min})) & ; \quad r < r_{vc}^{\min} \end{cases} \\ g_{vv}(r) &= g_{vv}^{mix}(r;\rho_v,d,\rho_c,d_c) \end{aligned} \qquad (5)$$

where g^{mix} is the radial distribution function for a hard sphere mixture with the average density of the background vapour $\rho_v = \rho_b - M\rho_c$, and a minimum cutoff in the radius, $r^{\min}$, is used equal to the radius where the effective potential has a maximum. The local density of the background vapour is $\rho_g = \rho_v/\xi$. In all cases, hard sphere functions are obtained from Rosenfeld's fundamental measure density functional theory. Finally, the effective pair interactions are

$$U_{cc}^{eff}(|\mathbf{R}-\mathbf{R}'|) = \int d\mathbf{r}d\mathbf{r}'\, P_c(\mathbf{r}-\mathbf{R})\phi_{SALR}(\mathbf{r}-\mathbf{r}')P_c(\mathbf{r}'-\mathbf{R}')$$
$$U_{vc}^{eff}(|\mathbf{R}-\mathbf{R}'|) = \int d\mathbf{r}'\phi_{SALR}(\mathbf{R}-\mathbf{r}')P_c(\mathbf{r}'-\mathbf{R}') \quad (6)$$

For this work a one-component SALR system is chosen for which the low density cluster fluid phase behaviour is known, corresponding to that used in earlier work[28]; A_a = 1.8, z_a = 1.0, A_r = 0.5, and z_r = 0.5.

Figure 1 shows the variation of the Helmholtz free energy for this system predicted by this thermodynamic model with reduced volume $V = (50)^3$. Six scenarios are considered; systems of 3125, 3250 and 3375 particles with only one or two clusters respectively. Results are plotted against the total number of particles within clusters and shifted so that the minimum of the single-cluster free energy is zeroed in each case.

We see a minimum in the free energy for both one and two-cluster states. The free energy is nearly symmetric about this minimum, except that for small clusters a maximum is reached corresponding to the critical nucleus size, while for increasingly large clusters it diverges. The horizontal lines are the free energy for a system without any clusters at the same overall system density. Thus, the single cluster nucleation barrier is equivalent to the free energy difference between the maximum of the single cluster system for small cluster sizes and the uniform fluid at the same overall density.

Let's consider the system with 3125 particles first. Initially, before any clusters are formed, there exists a considerable free energy barrier, of height 44.5 k_BT, against nucleation of the first giant cluster. However, once the first cluster forms the free energy minimum for a single cluster is also quite deep. Therefore, the one-cluster state is stable. The solution with two clusters is much less stable. In principle it can occur, but it will be rare and thermodynamically unstable with respect to a single cluster.

By increasing the number of particles to 3250 we see that the nucleation barrier is reduced only slightly to 42.5 k_BT, but the free energy minimum of the one-cluster

state is now somewhat deeper. However, the two cluster state is now marginally stable compared to the one-cluster state, although these states are separated by a free energy barrier. By the time the system reaches 3375 particles, the two cluster state is easily the more stable, although it is separated from the one cluster state by a free energy barrier. Once the two cluster state is formed, the one-cluster state will occur only rarely. Let us suppose that the number of particles in the system is gradually increased from 3125 to 3375 so slowly that the system always remains at or near its equilibrium state. At some point between these two limits the two-cluster system becomes more thermodynamically stable, and we should expect to observe a transition from one to two giant clusters.

The key issue under discussion in this work concerns how this transition takes place. There are two possibilities. Either a nucleation event occurs or the single cluster divides into two, i.e. a reproduction event occurs. To understand which process dominates we need to consider the respective free energy barriers for these transitions. If the free energy barrier for reproduction is much less than the free energy barrier for nucleation, then we can expect reproduction will dominate. Let's consider the system with 3250 particles, i.e. just after the equilibrium transition point. We know already the free energy barrier for nucleation of the first cluster from a uniform dispersion with 3250 particles is around 42.5 k_BT. However, the free energy barrier for nucleation of the second cluster after the first one has formed is even larger, because after nucleation of the first cluster the vapour density surrounding the single cluster has reduced and it is from this low density vapour that the second cluster must nucleate.

In fact, at the transition point where the two phase branches cross, denoted by a circular symbol in Figure 1, the vapour surrounding the first cluster has reduced to a density of 0.02092 from 0.026 when there are no clusters. We can therefore estimate the

free energy barrier for nucleation of the second cluster using the free energy model by considering nucleation from this lower density vapour. The two cases, one with uniform vapour density of 0.02092 and the other with a single giant cluster at the same overall system density, are shown in Figure 2. As we expected, the nucleation barrier for the second cluster is higher, at 48 k_BT.

To estimate the nucleation barrier for reproduction we can investigate the one and two-cluster states at the transition point where the two phase branches cross in Figure 1. Clearly, at this transition point these systems have the same number of particles overall, and the same number of particles within the clusters. In addition, the thermodynamic model predicts they have the same background vapour density (0.0198), and almost the same cluster internal body density (0.751 vs 0.752) for one and two clusters respectively. They thus have almost the same total cluster volume. Therefore, to transform from the one to two-cluster state, essentially all that need happen is the single cluster 'morphs' without any significant particle transfer between cluster and background vapour, or any significant change in cluster volume. This can be achieved by first transforming from a sphere to a 'sausage' shape (a cylinder with hemispherical ends), and then by 'pinching' in the middle to form two individual spherical clusters. Geometrically, there is a significant change in the interfacial area of the liquid-like cluster/s during this transformation. But since it takes place without any change in Helmholtz free energy, we can conclude that the surface tension during this transition is essentially zero, because the surface tension is defined as the rate of change of free energy with interfacial area, under suitable constraints. In other words, the one to two-cluster transition takes place when the one-cluster state approaches zero interfacial tension. We can therefore expect that the free energy barrier between the one and two-cluster states is similar to that shown in Figure 1, i.e. about 10 k_BT at the transition. This

relatively small free energy barrier will decrease quickly as the number of particles in the one-cluster system continues to increase past the transition point. When compared to the free energy barrier for *nucleation* of the second cluster, we can see that cluster reproduction is expected to dominate.

IV. Monte Carlo simulation of Giant SALR cluster reproduction

In the previous section we used a thermodynamic model to predict the relative rates of two processes in the presence of an existing giant SALR cluster; cluster reproduction versus cluster nucleation. We saw that, according to the theory, cluster reproduction is expected to dominate. Moreover, this thermodynamic model predicts this behaviour is universal for these giant SALR clusters, i.e. it is not a special case for the set of SALR parameters chosen.

To investigate whether this outcome is an artefact of the theory this prediction is tested by comparison with simulations. Brownian dynamics is a suitable method for simulating molecular and colloidal dispersions in dense solvents, which are the type of soft matter systems generally represented by the effective SALR potential. But such methods struggle to deal with hard core particles, as are used here. Fortunately, it has been shown[36,37] that the standard Metropolis Monte Carlo method, which is able to treat hard core particles, reproduces the collective dynamical properties of Brownian dynamics simulations quite accurately for spherical particles provided only single particle moves with small displacements are allowed. It is then possible to define an effective time-step[37], if desired, corresponding to a Monte Carlo step, and such simulations belong to a class of 'dynamic Monte Carlo' simulation method[38]. Moreover, the aim here is to allow for a very slow increase in the number of particles in a fixed simulation volume, which might correspond experimentally to slowly concentrating the

solution through solvent evaporation, for example. Again, a standard Monte Carlo method, namely Grand Canonical Monte Carlo (GCMC) should suffice to reproduce this behaviour, provided the rate of trial particle insertions and deletions is sufficiently slow. Indeed, as the intention is to allow for only a gradual *increase* in the number of particles, and we are not actually interested in equilibrating the system at a given chemical potential, only trial GCMC insertions need be performed at a fictitious chemical potential – trail deletions are unnecessary. Therefore, a standard type of GCMC method, where trail deletions are never performed, should be an adequate method for determining the average system dynamics of such solute dispersions, provided only small particle displacements are made, there are no 'special' or non-physical Monte Carlo moves, and trial insertions are suitably rare.

The length of a simulation is measured in terms of cycles, where a cycle consists of an attempt to move each particle and possibly an attempt to insert one particle. A cubic simulation box of side length 50, with periodic boundaries in each direction, and a long-ranged cutoff of half the box length is employed. Only trial displacements with a maximum length of 0.35 are allowed and the fictitious fugacity, sufficient for reasonable particle insertion acceptance rates, is set to 0.016. The same SALR parameters are used as before, i.e. $A_a = 1.8$, $z_a = 1.0$, $A_r = 0.5$, and $z_r = 0.5$. To ensure that between trial particle insertions simulations are maintained very close to equilibrium, the rate of insertion attempts must be held very low. To determine a suitable rate, simulations are performed with a range of trail insertion frequencies. Behaviour should converge to a characteristic type as the rate is reduced.

Because the aim here is to determine the system's behaviour in the presence of an existing cluster, an initial simulation is used to generate a starting configuration consisting of a single giant cluster. This initial simulation began with 2000 particles

randomly placed in the cubic simulation box, with trail particle insertions every 1000 cycles. After 100,000 cycles a single giant SALR cluster formed. This configuration is used as input to the following simulations.

Figure 3 displays a series of snapshots from three further Monte Carlo simulations, all initialized with the same single-cluster configuration as described above, corresponding to trial insertions every 100, 300, and 1000 cycles. In Figure 3a, corresponding to one insertion attempt per 100 cycles, we see that a second cluster nucleates just before 125,000 cycles, and then a third cluster nucleates just before 225,000 cycles. After this, each cluster continues to grow, eventually forming sausage-shaped clusters. This simulation shows that a rate of one insertion attempt per 100 cycles is too high to maintain the system sufficiently close to equilibrium for reproduction to occur. Instead, the rate at which particles accumulate in the dispersed phase is higher than the rate at which particles can diffuse to existing clusters. Therefore, the dispersed phase becomes over-concentrated, and nucleation is preferred.

In Figure 3b, corresponding to one insertion attempt per 300 cycles, we do not see any nucleation or reproduction events. Instead, the existing cluster continues to grow, eventually forming a very long sausage-shaped cluster that spans the simulation box. This occurs because now the rate of accumulation of particles in the dispersed phase is lower than the rate of diffusion to the existing cluster. However, the rate of diffusion to the existing cluster from the dispersed phase exceeds the rate of diffusion of particles within the cluster. Therefore, the cluster cannot internally equilibrate and reproduce, and instead continues to grow.

Finally, in Figure 3c, corresponding to one insertion attempt per 1000 cycles, we only see reproduction events, without any nucleation events. The first reproduction event takes place just before 600,000 cycles, and then the lower daughter reproduces

just after 1 million cycles, while the other daughter reproduces just before 1.6 million cycles. Reproduction occurs here because the rate of diffusion of particles from the dispersed phase to existing clusters, and the rate of diffusion within clusters, is faster than the rate at which particles accumulate in the system. In other words, the rate of accumulation of particles is sufficiently slow that the system can remain sufficiently close to equilibrium for reproduction to occur. This supports the theoretical prediction.

Essentially, existing clusters act as nucleation centres for production of further clusters. In reference [28] we saw many giant clusters nucleate simultaneously within a canonical ensemble simulation. That occurred because the system was deliberately initiated with a substantially over-saturated initial state, i.e. a massive excess of particles above the CCC. This is not the case here. Here, the system is initiated either below or only slightly above the CCC. Therefore, only a single cluster nucleation event is observed initially, with reproduction dominating afterwards provided the rate of accumulation of particles is sufficiently slow.

V. Potential for chemical evolution of giant SALR clusters

The basis of biological evolution is self-replication together with random genetic changes between generations and fitness selection[39]. Changes to the genetic code can lead to a wide range of potential and actual genetic life forms. Those life forms best suited to the changing environment are able to proliferate more quickly, and are said to be successful. The less successful life forms are out-competed for resources and therefore become evolutionary dead-ends.

Biological genetic evolution has inspired many powerful numerical optimisation algorithms, successful across science and engineering. The general process for these evolutionary algorithms mirrors the basic genetic evolutionary steps of biology[40]. First,

a new population is created from the preceding one by performing simple random operations on their ‘genetic’ information. Next, the fitness of all members of the population is assessed. The fitter members of the population are selected (survive) while the less fit are discarded (die). The cycle then repeats. Any process that has these repeating steps, i.e. self-replication with small random changes followed by selection of the fitter members, leads to an optimisation process. Here, this is referred to as ‘evolution’.

The simulations and theoretical results just described demonstrate that giant SALR cluster growth and reproduction can occur in SALR fluids in preference to nucleation events provided the rate of accumulation of particles is sufficiently slow. However, these simulations and the theory involve only one solute component. By definition, chemical evolution is absent. Clearly, fitness selection is also absent. What can we expect to observe in dispersions of several components, where there is at least one SALR component? As for any phase equilibrium involving mixtures, we can expect additional components to partition between the dispersed phase and liquid-like cluster phases. That is, we can expect clusters to be internally mixed with a wide range of possible compositions. Depending on the miscibility of each component within clusters, and the various interfacial tensions, we might also expect more than one type of cluster to occur, or to observe structured clusters (e.g. core-shell types).

However, such systems remain relatively simple. Chemical reactions, interfaces, physical agitation, gravity, and chemical potential, pressure and temperature gradients are some of the more important ingredients that could be included. Chemical reactions in particular are necessary to generate a diversity of increasingly complex chemical components required for giant SALR cluster evolution. An important feature of these systems is that the rate of reaction between components within giant clusters would be

increased, relative to the dispersed state, due to the enhanced concentration of chemicals within clusters. Therefore, each cluster could be considered a nano/microscale chemical reactor, in much the same way as modern cells.

However, an optimised process of chemical evolution of giant SALR clusters requires more than just cluster growth and reproduction, even allowing for chemical reactions. It is essential that the information content (chemical composition and any secondary and higher order structures) of a cluster is preserved with only minor changes between generations. Modern cells achieve this fundamentally through the use of very complex auto-catalytic reaction networks and bilayer lipid cell membranes. Complex auto-catalytic reaction networks ensure the reproduction of chemical information within cells with high precision, while lipid cell membranes ensure this information is only transferred between cells via reproduction. It is not known whether both of these features are strictly required to enable the chemical evolution of giant SALR clusters. That is, simple auto-catalytic reaction networks embedded within giant SALR clusters without lipid membranes might suffice. Future work will aim to test this hypothesis. Finally, if through chemical evolution giant SALR clusters become so chemically complex that functioning clusters cannot be formed through nucleation in a reasonable time, yet they can still form through reproduction in a reasonable time, then might these clusters be said to exhibit ‘death’, and therefore perhaps also ‘life’?

VI. Conclusions

It is demonstrated here that giant SALR clusters can ‘reproduce’. Essentially, when the system concentration increases sufficiently slowly, such as might be achieved through the gradual evaporation of solvent, giant clusters serve as nucleation centers for the production of further clusters, in preference to homogeneous nucleation. For chemical

mixtures able to undergo reactions that also display giant SALR clusters, chemical evolution of clusters might be observed in suitable systems with evaporation cycles. Future work will aim to test this hypothesis using *in-silico* methods. This observation could have profound consequences for a wide range of soft matter systems.

Acknowledgements: I thank Laura Machesky and Robert Insall for some helpful discussions.

References

[1]J. Groenewold and W. K. Kegel, Journal of Physical Chemistry B **105**, 11702 (2001).

[2]F. Sciortino and P. Tartaglia, Advances in Physics **54**, 471 (2005).

[3]A. J. Archer and N. B. Wilding, Physical Review E **76**, 031501 (2007).

[4]J. Groenewold and W. K. Kegel, Journal of Physics-Condensed Matter **16**, S4877 (2004).

[5]N. Schunk and L. M. Robledo, Reports on Progress in Physics **79** (2016).

[6]A. Stradner, H. Sedgwick, F. Cardinaux, W. C. K. Poon, S. U. Egelhaaf, and P. Schurtenberger, Nature **432**, 492 (2004).

[7]A. I. Campbell, V. J. Anderson, J. S. van Duijneveldt, and P. Bartlett, Physical Review Letters **94**, 208301 (2005).

[8]R. Sanchez and P. Bartlett, Journal of Physics-Condensed Matter **17**, S3551 (2005).

[9]E. Stiakakis, G. Petekidis, D. Vlassopoulos, C. N. Likos, H. Iatrou, N. Hadjichristidis, and J. Roovers, Europhysics Letters **72**, 664 (2005).

[10]R. P. Sear, Current Opinion in Colloid & Interface Science **11**, 35 (2006).

[11]A. Stradner, F. Cardinaux, and P. Schurtenberger, Journal of Physical Chemistry B **110**, 21222 (2006).

[12]F. Cardinaux, A. Stradner, P. Schurtenberger, F. Sciortino, and E. Zaccarelli, Epl **77**, 48004 (2007).

[13]N. Javid, K. Vogtt, C. Krywka, M. Tolan, and R. Winter, Physical Review Letters **99**, 028101 (2007).

[14]F. J. Zhang, M. W. A. Skoda, R. M. J. Jacobs, R. A. Martin, C. M. Martin, and F. Schreiber, Journal of Physical Chemistry B **111**, 251 (2007).

[15]N. Destainville, Physical Review E **77**, 011905 (2008).

[16]A. C. Dumetz, A. M. Chockla, E. W. Kaler, and A. M. Lenhoff, Biophysical Journal **94**, 570 (2008).

[17]A. Shukla, E. Mylonas, E. Di Cola, S. Finet, P. Timmins, T. Narayanan, and D. I. Svergun, Proceedings of the National Academy of Sciences of the United States of America **105**, 5075 (2008).

[18]F. Bordi, S. Sennato, and D. Truzzolillo, Journal of Physics-Condensed Matter **21**, 203102 (2009).

[19]N. Kovalchuk, V. Starov, P. Langston, and N. Hilal, Advances in Colloid and Interface Science **147-48**, 144 (2009).

[20]J. C. F. Toledano, F. Sciortino, and E. Zaccarelli, Soft Matter **5**, 2390 (2009).

[21]F. Cardinaux, E. Zaccarelli, A. Stradner, S. Bucciarelli, B. Farago, S. U. Egelhaaf, F. Sciortino, and P. Schurtenberger, Journal of Physical Chemistry B **115**, 7227 (2011).

[22]K. Larson-Smith and D. C. Pozzo, Soft Matter **7**, 5339 (2011).

[23]K. P. Johnston, J. A. Maynard, T. M. Truskett, A. U. Borwankar, M. A. Miller, B. K. Wilson, A. K. Dinin, T. A. Khan, and K. J. Kaczorowski, Acs Nano **6**, 1357 (2012).

[24]T. H. Zhang, J. Klok, R. H. Tromp, J. Groenewold, and W. K. Kegel, Soft Matter **8**, 667 (2012).

[25]S. Kumar, M. J. Lee, V. K. Aswal, and S. M. Choi, Physical Review E **87**, 042315 (2013).

[26]A. K. Murthy, R. J. Stover, A. U. Borwankar, G. D. Nie, S. Gourisankar, T. M. Truskett, K. V. Sokolov, and K. P. Johnston, Acs Nano **7**, 239 (2013).

[27]Y. Zhuang and P. Charbonneau, Journal of Physical Chemistry B **120**, 7775 (2016).

[28]M. B. Sweatman, R. Fartaria, and L. Lue, Journal of Chemical Physics **140**, 124508 (2014).

[29]M. B. Sweatman and L. Lue, Journal of Chemical Physics **144**, 171102 (2016).

[30]A. Ciach and O. Patsahan, Condensed Matter Physics **15**, 23604 (2012).

[31]J. M. Bomont, J. L. Bretonnet, D. Costa, and J. P. Hansen, Journal of Chemical Physics **137**, 011101 (2012).

[32]A. Ciach, Physical Review E **78**, 061505 (2008).

[33]S. F. Banani, H. O. Lee, A. A. Hyman, and M. K. Rosen, Nature Reviews Molecular Cell Biology (2017).

[34]A. Ciach and W. T. Gozdz, Condensed Matter Physics **13**, 23603 (2010).

[35]A. J. Archer, C. Ionescu, D. Pini, and L. Reatto, Journal of Physics-Condensed Matter **20**, 415106 (2008).

[36]D. M. Heyes and A. C. Branka, Molecular Physics **94**, 447 (1998).

[37]E. Sanz and D. Marenduzzo, Journal of Chemical Physics **132** (2010).

[38]A. Cuetos and A. Patti, Physical Review E **92** (2015).

[39]B. R. Johnson and S. K. Lam, Bioscience **60**, 879 (2010).

[40]M. Mitchell, *An introduction to genetic algorithms*. (MIT Press, 1996).

Figures

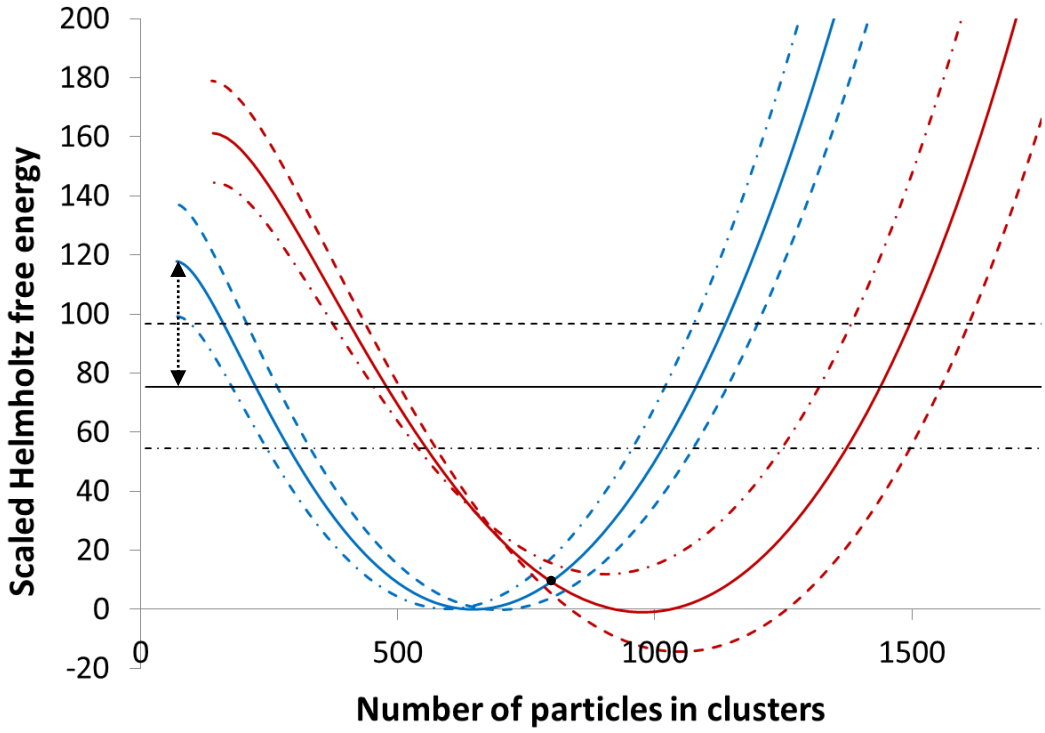

Figure 1. Shifted Helmholtz free energy for giant SALR clusters in a volume of $(50)^3$ for an SALR system (see text) with $A_a = 1.8$, $z_a = 1.0$, $A_r = 0.5$, $z_r = 0.5$, as predicted by the thermodynamic model of reference [28]. The curved lines correspond to; blue – one cluster, red – two cluster, systems with 3125 (dash-dot lines), 3250 (full lines) or 3375 (dashed lines) particles in total (corresponding to reduced densities of 0.02575, 0.026, and 0.02625 respectively). Horizontal lines indicate the free energy of the uniform fluid (without giant clusters) relative to the one-cluster case. The arrow indicates the predicted free energy barrier for nucleation of the first cluster. The small circle indicates the approximate free energy barrier height for the one-cluster to two-cluster transition.

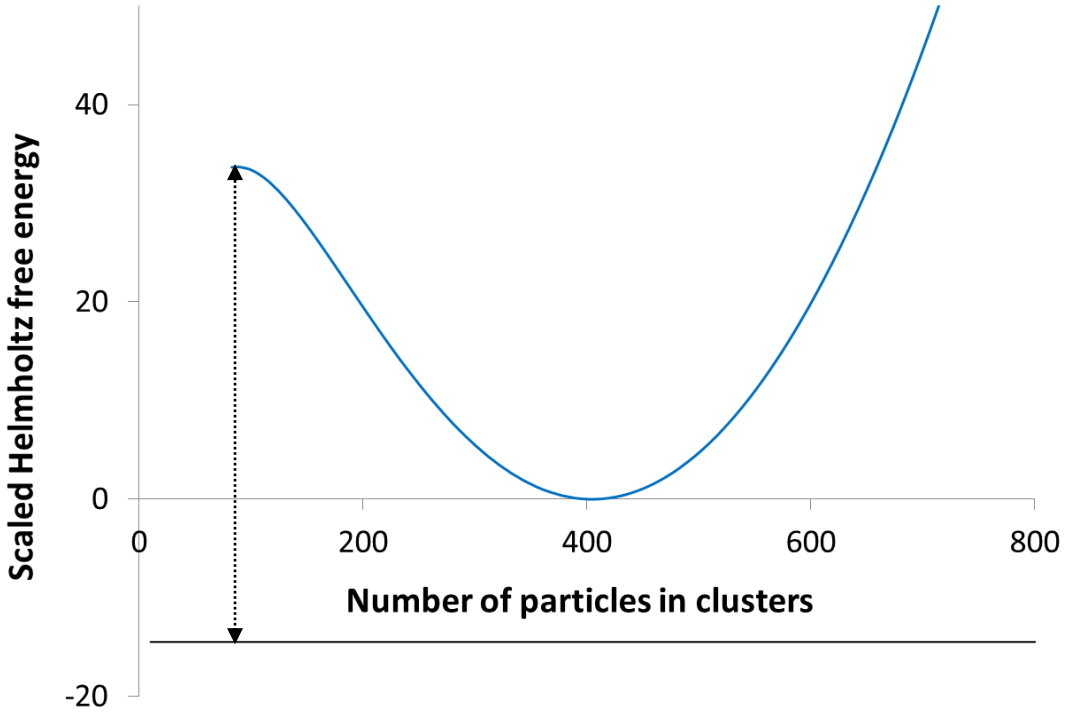

Figure 2. As for Figure 1, except for a reduced density of 0.02092, corresponding to 2615 particles. The arrow indicates the approximate free energy barrier for nucleation of the second cluster.

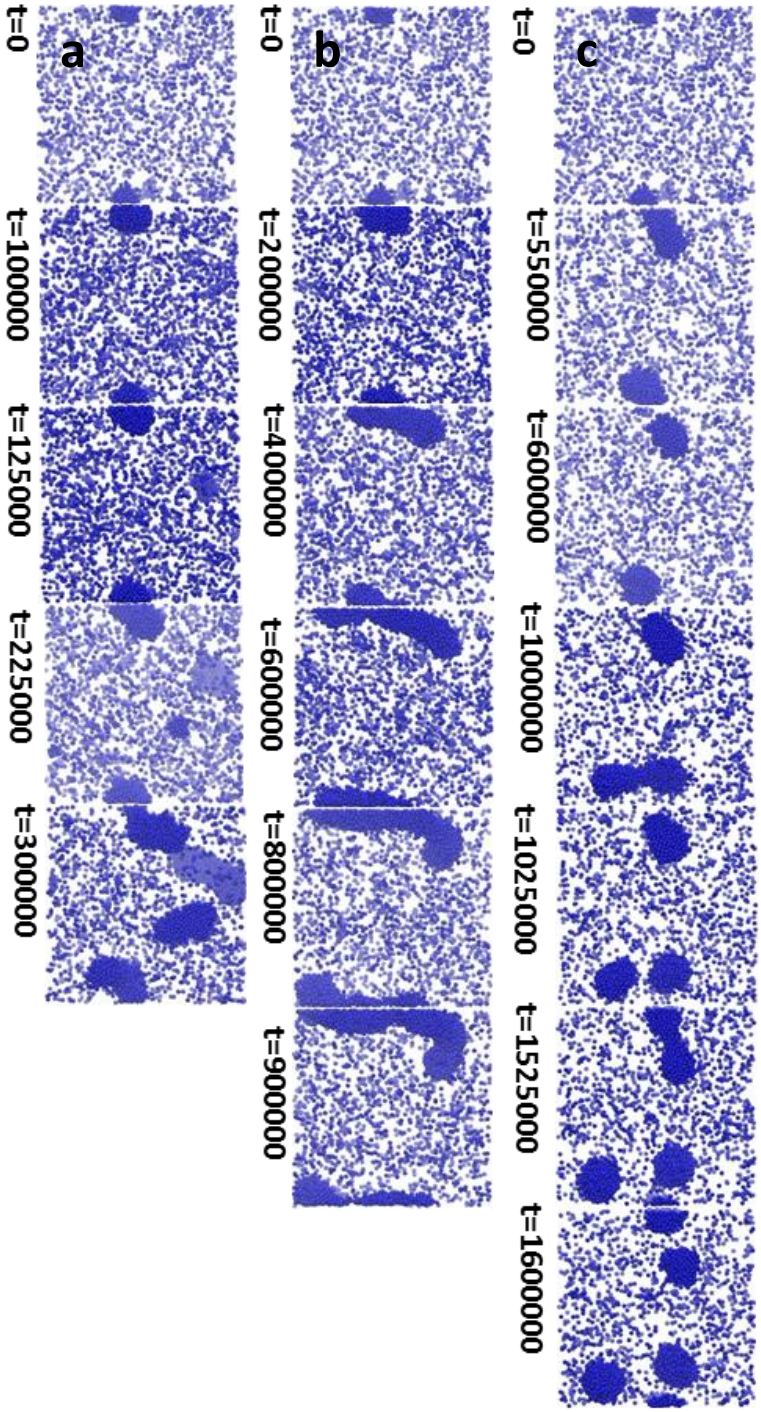

Figure 3. Snapshots from Monte Carlo simulations illustrating giant SALR cluster growth and reproduction, where t is the number of Monte Carlo cycles performed. Simulations are initiated from the same configuration with one large cluster, where A_a = 1.8 (see text). The three simulations have a) one insertion attempt per 100 cycles, (b) one insertion attempt per 300 cycles, and c) one insertion attempt per 1000 cycles.